J. Comp. App. Res. Mech. Eng. Vol. 15. No. 2, pp. 199-207, 2026 *DOI: 10.22061/jcarme.2026.12353.2702*

Journal of Computational and Applied Research in Mechanical Engineering
jcarme.sru.ac.ir
SRTTU
JCARME
ISSN: 2228-7922

Research paper

Failure analysis of St12 steel during expansion forming by SCDA: a combined finite element and experimental approach

S. A. Alavi[a], S. M. H. Seyedkashi[a,*] and M. Rakhshkhorshid[b]

[a]*Department of Mechanical Engineering, University of Birjand, Birjand, South Khorasan, 97175-376, Iran*
[b]*Department of Mechanical and Materials Engineering, Birjand University of Technology, Birjand, South Khorasan, 9719866981, Iran*

Article info:

Article history:

Received: 04/08/2025
Revised: 23/07/2026
Accepted: 25/07/2026
Online: 27/07/2026

Keywords:

SCDA expansion forming,
Soundless chemical demolition agent,
Finite element analysis,
Volume expansion,
Crack growth.

[*]Corresponding author:
seyedkashi@birjand.ac.ir

Abstract

This study investigates crack formation and rupture in a newly developed "SCDA expansion forming", which utilizes the pressure generated by a soundless chemical demolition agent (SCDA). The research integrates experimental analysis and finite element analysis (FEA) to examine the forming of a 1 mm thick St12 low-carbon steel sheet into a dome shape. The experimental phase involved using Green Rock SCDA within a rigid steel die under test conditions of 75°C temperature, 25% water content, and 300 g mixture mass. The corresponding FEA was performed in Abaqus, applying the forming limit diagram (FLD) damage model criteria to predict necking instability and crack formation. The results from both the simulation and the experimental tests demonstrated that rupture occurs in the areas between the dome's center and its corners. FEA revealed that the maximum plastic strain and stress are concentrated in these central regions, leading to localized thinning and eventual failure. The experimental findings confirmed the location of the crack, thereby validating the accuracy of the numerical model. Analysis of the fracture surface via scanning electron microscopy (SEM) indicated a ductile fracture mechanism, characterized by dimples formed through a combination of shear and tensile modes.

1. Introduction

With the advancement of technology in modern industries, manufacturing processes have also changed or been modified to improve the dimensional accuracy of manufactured parts, increase production speed, and reduce costs.
Among manufacturing processes, forming processes have gained a special position due to their simplicity, suitability for a wide range of products, increased strength and durability of manufactured parts, wide application, greater efficiency, less waste, time and cost savings, production of complex geometric shapes, etc. [1].
Recently, a new forming method, known as “SCDA expansion forming”, has been proposed by the authors in which the expansion pressure generated by a soundless chemical demolition agent (SCDA) is utilized to form sheet metals

[2]. The advantages of this method compared to other forming methods include reduction of production steps, no need for expert personnel, less risk of danger, less cost, lower noise pollution, availability of SCDA, simple and inexpensive equipment, no special environment, and no damage to the environment.

SCDAs are in powder form, usually used in the fragmentation of underground rock and demolition of buildings [3, 4]. The demolition process is performed under expansive pressure created by the hydration of SCDAs. Calcium oxide (CaO) is the main expansive ingredient in SCDA. However, other materials are also combined for the hydration process.

When SCDA reacts with water, its volume expands up to 2–3 times according to Eq. (1) [4]:

$$CaO + H_2O \rightarrow Ca(OH)_2 + 15.2 \uparrow (\frac{kCal}{mol}) \quad (1)$$

In this reaction, significant expansion pressure is generated due to the hydration of CaO and the formation of $Ca(OH)_2$. When the generated stresses reach the tensile strength of the materials, cracks are formed and propagate in the surrounding materials [5].

The volumetric expansion of SCDAs occurs in two stages. In the first stage, the volumetric expansion is usually fast, but it is relatively slow in the second stage [2]. Unlike explosives, which produce high pressure in a very short time, the SCDA produces high pressure over an extended period of time [6]. The created pressure is significantly influenced by the amount of SCDA, water content, and ambient temperature [2, 7]. Gui *et al.* [8] examined the effect of subsequent heating on the expansive pressure of SCDA and reported that the temperature and pressure increase suddenly after heating. Li *et al.* [9] investigated the static expansion tensile behavior of concrete after exposure to elevated temperatures and stated that the changes in surface features after being treated at high temperatures are related to the physical properties.

Hinze and Brown [10] studied the properties of SCDA using a test setup consisting of thick-walled steel cylinders. They found that the most important parameters affecting the expansive pressure are the water percentage and the ambient temperature. They also noted that when the ambient temperature increased to 30°C, the expansion pressure rose to more than 100%. Huynh [11] investigated the destruction of unreinforced concrete blocks by SCDA and reported that an increase in environmental temperature by 3°C decreased the expansion onset time by about 4 hours. Laefer *et al.* [4] examined the effect of thermal transfer on the SCDA. They found that by quadrupling the volume of SCDA in a pipe at 10 ºC, the peak hydration onset accelerated and the expansive pressure increased by up to 700%. Also, Laefer *et al.* [12] reported that the ambient temperature, amount of mixing water, hole diameter, and hole depth are effective parameters on the expansion pressure of the SCDA.

The increasing development of technology in simulation software allows researchers to numerically analyze and examine the forming process before implementation, which saves time and money.

One of the most important issues in the forming processes is the formation of cracks and tears in the sheet, which is usually investigated using the finite element analysis (FEA) technique. Since SCDA mixtures expand equally in all directions, the modeling of the forming process using SCDA is similar to hydroforming.

Yapan *et al.* [13] used Johnson-Cook's hardening and damage model to investigate the failure of the Ti-6Al-4V alloy in the hydroforming process and observed that the fracture zones exhibited good agreement with the experimental results. Hashemi *et al.* [14] proposed an adaptive FEA to design bimetal cup hydroforming. Hambli [15] used different damage models to simulate crack growth during the blanking process and reported that the Gurson damage model is not able to predict the fracture propagation path realistically. El-Aty *et al.* [16] performed FEA of the hydroforming process to predict the forming limit and thickness distribution of 304 stainless steel.

The FEA of the hydroforming process was also implemented by Ahamed *et al.* [17], Alizad-Kamran [18], Hashemi *et al.* [19], and Jebri *et al.* [20]. Finite element analysis of the forming process using SCDA is also similar to the Nakajima method for obtaining the sheet

forming limit, which has been investigated by many researchers. Marquez-Monje *et al.* [21] used the FEA technique to analyze the formation of cracks during the Nakajima tests. They observed that microperforated samples oriented in transversal and longitudinal orientations have similar cracks, while the samples placed in the diagonal direction of the crack were different. Komori and Matsushima [22] used an ellipsoidal void model to predict ductile fracture during Nakajima tests and found that the fracture forming limit calculated using the ellipsoidal void model agreed closely with that obtained from the experiment. Xue *et al.* [23] simulated the Nakajima test using the FEA to predict the FLD of Mg-AZ31 and Al-7050 alloys. Jalil *et al.* [24] studied the forming limit of sheets into shell conical parts using a hydrodynamic deep drawing process assisted by radial pressure. The FEA for predictions of FLD was also studied by Meragalge *et al.* [25], Nakwattanaset and Suranuntchai [26], Shahzamanian *et al.* [27], Zhang [28], and Yang and Huang [29].

Based on the literature, this newly introduced forming process has been developed for the first time by the authors in the previous work on SCDA expansion forming [2]. Its primary goal was to introduce the "SCDA expansion forming" method as a viable manufacturing process. That research focused on a parametric study (ANOVA) to understand how inputs (ambient temperature, water content, mixture mass) affect the outputs (volumetric expansion, onset time).

The present research builds directly on the foundation of Ref. [2], using the optimized process as a case study to understand how, where, and why failure occurs. It extends the previous work by moving from process observation to failure prediction, using damage initiation and stress criteria in the simulation to pinpoint the location of crack formation. It provides a deep fractographical analysis via SEM to characterize the micro-scale failure mechanism (ductile fracture, dimple formation.

2. Materials and methods

In this research, the commercial Green Rock SCDA has been used (Table 1). The drinkable tap water is used to mix with SCDA. The forming process has been carried out on a 1 mm thick St12 low-carbon steel sheet. The mechanical properties for St12 were obtained by the standard tensile test, which are presented in Fig. 1(a) and Table 2. Also, it should be mentioned that as the as-received material was an annealed sheet metal, it was considered an isotropic material in the simulation. The forming limit diagram (FLD) obtained from the Nakajima test is presented in Fig. 1(b). More details about extracting the FLD through the Nakajima test can be found in Alavi *et al.* [2].

Table 1. Technical specifications of Green Rock.

Physical state	Color	Special Weight	Ability to dissolve
Powder	Grey	1.4 ton/m^3	Soluble in water

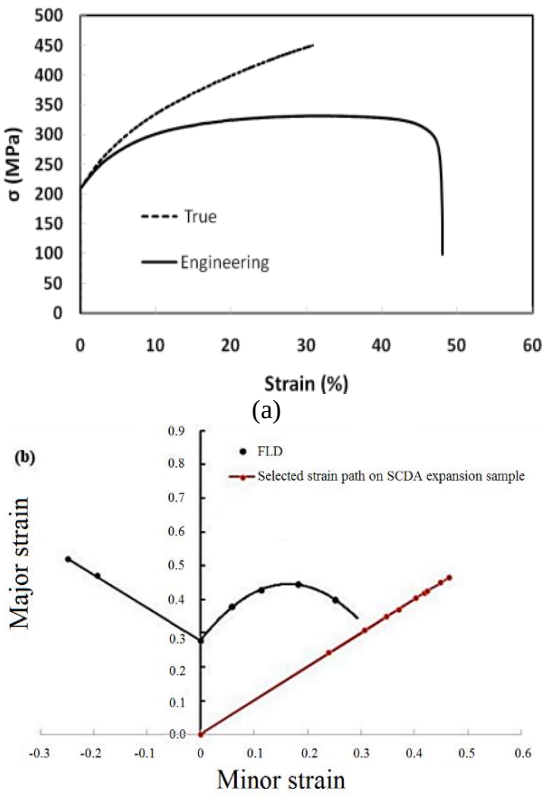


Fig. 1. (a) Stress-strain diagram obtained from the tensile testing and (b) FLD diagram of St12 steel [2].

Table 2. Mechanical properties of St12 steel.

Ultimate tensile strength (MPa)	Yield strength (MPa)	Uniform elongation (%)	Total elongation (%)	Elastic modulus (GPa)
364	232	34	47	230

To mix SCDA with water, a clean, grease-free plastic container was used. In order to weigh the SCDA powder and water, a digital scale (ATG model) with a measurement resolution of 0.1 g and automatic calibration capability was used. It is worth mentioning that the largest volume of SCDA is obtained at the maximum hydration temperature.

Based on the previous research [2], the test condition was determined as a temperature of 75°C, a water percentage of 25%, and a mixture mass of 300 g.

An appropriate setup was designed to manufacture a dome-shaped sheet metal part using SCDA powder. It was observed that during the forming process, SCDA exerts high pressure in different directions. Therefore, it is required to design and manufacture a rigid die with high strength.

The die designed for volumetric expansion forming with SCDA is made of Ck45 steel with a thickness of 25 mm. Fig. 2(a) shows the designed die assembly. After forming the steel sample, the surface of the crack was analyzed by scanning electron microscopy (SEM, VEGA-TESCAN-XMU model).

In this study, the FE simulation method is used to simulate the sheet forming process using the expansion pressure caused by SCDA. The simulation of the forming process is carried out by the Abaqus software. In Abaqus software, the sheet is introduced as a shell-deformable, and the die components are rigid.

The FLD damage model was used in this study to predict the onset of necking instability and the crack formation in sheet metal. According to the literature review [7], it was recognized that the SCDA can exert a pressure of 150 to 185 MPa on the die and sheet. So, in this research, the applied pressure was considered to be 185 MPa. The die diameter was 105 mm, and the Coulomb friction model was applied between the die and sheet metal.

When the stress in the sheet reaches its ultimate strength in the simulation, the material absorbs energy, which is equal to the area under the stress-strain diagram up to UTS. At the failure location, due to the activation of the Status option in Abaqus, all elements that reach the failure zone are removed.

The Dynamic/Explicit solver is applied in the software because the sheet metal has a nonlinear behavior during the forming process. Two stages are performed to complete the forming process. First, a blank-holder force is applied to the sheet, and then the forming force is applied. In this process, the coefficient of friction is not very high; thus, it is considered to be 0.1.

The meshing method for the sheet metal and die is shown in Fig. 2(b). Triangular elements (Tri) with a size of 7 mm were applied to mesh the upper and lower dies. Moreover, the number of elements was 6028 and 16206 for the upper and lower dies, respectively. Three elements with a size of 3 mm were also used for the steel sheet. 11206 elements were selected for the sheet using the mesh convergence method.

3. Results and discussion

In order to validate the FE model, the experiments were conducted three times under the parameters of 75°C temperature, 25% water content, and 300 g mixture mass. During the expansion of the SCDA powder within the die, the sheet gradually deformed into a hemispherical shape. The same failure appearance was observed in all of them.



(a) (b)

Fig. 2. (a) Designed and manufactured die and (b) meshing of the sheet and die.

The hydration reaction's exothermic peak triggered rapid water evaporation, significantly accelerating the formation rate. This sudden temperature rise generated substantial internal pressure, which was effectively regulated through a strategically placed vent at the die's extremity. Fig. 3 shows both the SCDA forming mechanism and the fabricated samples.

It should be noted that during the initial stage of the process, both the volumetric expansion and temperature exhibit minimal changes. As time passed, a sudden increase in the temperature of the SCDA material occurred, reaching the peak hydration temperature [7].

The volumetric expansion of the sheet grows as the temperature rises, reaching its highest level at the maximum hydration temperature. The enhanced volumetric expansion at higher temperatures may result from the exothermic hydration reaction of CaO, which promotes the formation of $Ca(OH)_2$ [12].

Fig. 4 shows the formation of cracks and tears in the sheet for the experimental and simulated samples. It should be noted that in the experimental forming process, the sheet was initially completely transformed into a hemisphere, but the forming process was continued until rupture [7].

As can be seen in both experimental and simulated samples, rupture occurred in areas close to the center and between the dome tip and the corners of the sheet. It is worth mentioning that the SCDA material exerts pressure in both horizontal and vertical directions, which are almost the same according to previous research [4, 12]. This causes the pressure to be maximized in the area between the center and the edges of the sheet, because horizontal pressure is not applied to the center of the sheet at the end of the process. The research first explored the stress and strain distribution within the sheet during the SCDA material forming process to assess the FEA results. The distribution of plastic strain across the metal sheet after the forming process is indicated in Fig. 5.

It can be seen that the maximum strain has occurred in the central regions of the sheet. This phenomenon occurs due to the development of peak pressure in these transitional zones during the forming process [7, 12].



Fig. 3. Forming process by SCDA and the produced sample.

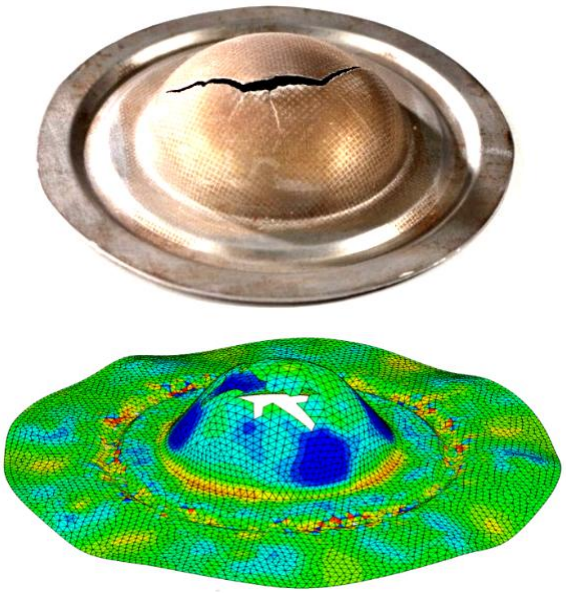


Fig. 4. Location of the crack in the experimental and simulated samples.

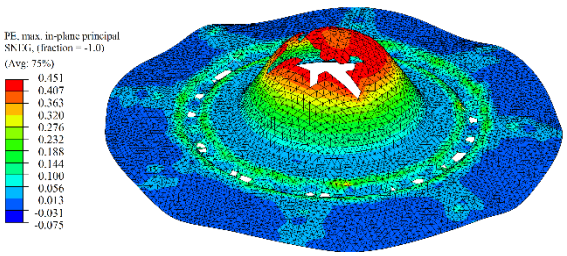


Fig. 5. Distribution of plastic strain in the sheet after rupture.

Therefore, the elements located in these areas reached the maximum stress and were eliminated, which led to the formation of cracks and tears in the sheet.

Fig. 6 presents the pressure distribution contours across various sheet regions. Notably, the SCDA

material exerts nearly equivalent pressure in both horizontal and vertical directions, as established in prior studies [4, 12].
This leads to peak pressure concentrations in the intermediate zone between the sheet's center and edges, as horizontal pressure diminishes in the central region during the final process stages. As evidenced in Fig. 6, the maximum plastic strain occurs at the sheet's center while the flange area shows minimal strain.
This distribution results from the center experiencing the greatest height increase and consequently undergoing more severe deformation than the peripheral regions [7]. To analyze the thickness variations in the formed sheet, Fig. 7 presents the thickness distribution contour after the forming process.
As expected, the minimum thickness occurred in the center of the sheet, which is due to the increased pressure in these areas [4, 7]. Therefore, the results obtained for the thickness distribution correspond to the location of the maximum plastic strain observed during the forming process.
As can be seen in Fig. 7, the reduction in thickness in the central areas of the sheet ultimately led to rupture. Fig. 8 shows the surface of the crack in the formed sample. SEM image of the fracture surface indicated that a ductile fracture had occurred. The ductile dimples exhibit a combination of shear and tensile modes of fracture propagation.
A ductile fracture generally involves the nucleation, growth, and coalescence of voids in a plastically deforming material. In many structural steels, void nucleation occurs at small strains and failure is controlled by void growth and coalescence [30].
Fig. 9 shows an SEM image of the crack surface with higher magnification. According to this figure, the steel appears quite clean with no inclusions or second-phase particles present at the bottom of the dimples.

4. Conclusions

This research successfully investigated the mechanisms of crack formation and rupture in soundless chemical demolition agent (SCDA) expansion forming.

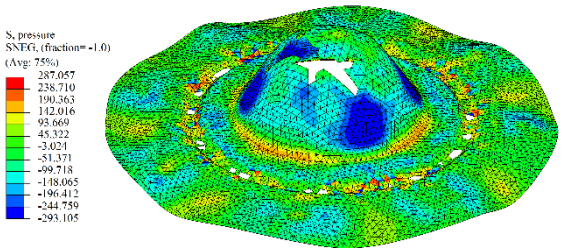


Fig. 6. Distribution of pressure in the sheet.

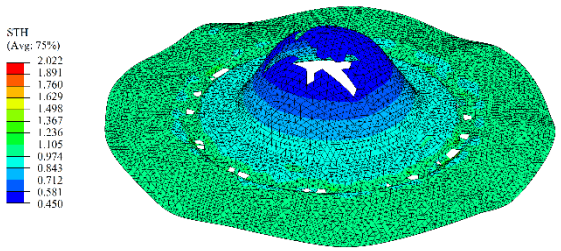


Fig. 7. Distribution of thickness in the sheet.

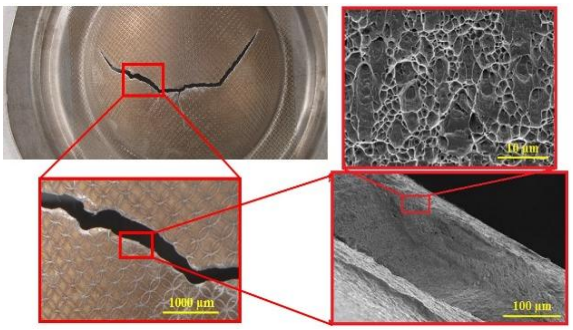


Fig. 8. Surface of the crack in the formed sample.

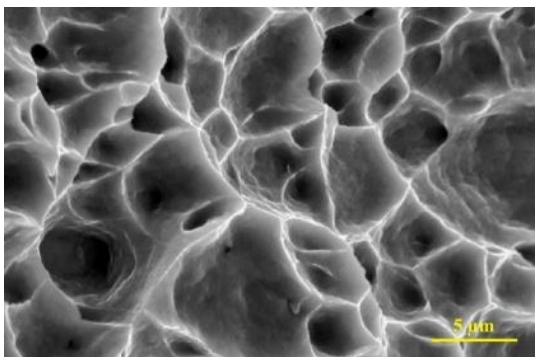


Fig. 9. SEM image of a crack in the formed sample.

A combined experimental and numerical approach was employed to analyze the forming of a 1 mm thick St12 steel sheet into a hemispherical dome.
The primary objective was to identify the location of failure and understand the underlying stress and strain conditions that precipitate it. The key findings demonstrate a strong

correlation between the finite element analysis and the experimental results.

The numerical simulation accurately predicted that the maximum plastic strain and stress would concentrate in the transitional zones between the dome's apex and its corners. This concentration, resulting from a unique pressure distribution where horizontal pressure diminishes centrally during the final stages of forming, leads to significant localized thinning and subsequent material failure.

The experimental tests validated these findings, with rupture consistently occurring in the same predicted regions. Further analysis of the fracture surface using scanning electron microscopy confirmed a ductile fracture mechanism, evidenced by the presence of dimples formed through a combination of shear and tensile loading.

The study confirms that the SCDA expansion forming process is a viable manufacturing technique whose failure modes can be reliably modeled. This foundational understanding of crack initiation and propagation provides a valuable framework for optimizing process parameters and expanding the application of this low-cost, simplified forming method.

Future work should further refine the numerical model by incorporating the dynamic effects of temperature and friction more explicitly.

References

[1] A. Awasthi, K. K. Saxena and V. Arun, "Sustainable and smart metal forming manufacturing process", *Mater. Today Proc.*, Vol. 44, No. 1, pp. 2069-2079, (2021).

[2] S. A. Alavi, S. M. H. Seyedkashi and M. Rakhshkhorshid, "A novel expansion forming process using soundless chemical demolition agent", *J. Mater. Eng. Perform.*, Vol. 34, No. 22, pp. 1-11, (2025).

[3] R. Li, Y. Yan, Z. Jiang, W. Zheng and G. Li, "Impact of hole parameters and surrounding constraint on the expansive pressure distribution and development in soundless chemical demolition agents", *Constr. Build. Mater.*, Vol. 307, No. 8, p. 124992, (2021).

[4] D. F. Laefer, A. S. Natanzi and S. M. I. Zolanvari, "Impact of thermal transfer on hydration heat of a soundless chemical demolition agent", *Constr. Build. Mater.*, Vol. 187, pp. 348–359, (2018).

[5] M. B. Étkin and A. E. Azarkovich, "Effect of non-explosive splitting compounds and rational work parameters", *Power Technol. Eng.*, Vol. 40, No. 5, pp. 287–292, (2006).

[6] J. Xu, "Investigation of non-explosive expansion material in roof caving field application", *Int. J. Rock Mech. Min. Sci.*, Vol. 120, pp. 50–57, (2019).

[7] A. S. Natanzi, D. F. Laefer and L. Connolly, "Cold and moderate ambient temperatures effects on expansive pressure development in soundless chemical demolition agents", *Constr. Build. Mater.*, Vol. 110, pp. 117–127, (2016).

[8] Y. Gui, Z. Jiang, C. Dai and Q. Zhang, "Enhanced effect of self-propagating subsequent heating on the expansive pressure on soundless chemical demolition agent", *Constr. Build. Mater.*, Vol. 364, p. 129866, (2023).

[9] X. Li, X. Xu, C. Wang, Z. Liu, Y. Chang and Q. Wang, "Experimental investigation of the static expansion tensile behavior of concrete after exposure to elevated temperatures", *Fire Technol.*, Vol. 59, No. 6, pp. 3667-3687, (2023).

[10] J. Hinze and J. Brown, "Properties of soundless chemical demolition agents", *J. Constr. Eng. Manag.*, Vol. 120, No. 4, pp. 816–882, (1994).

[11] M. P. Huynh, *Investigation of crack propagation due to expansion agents*, M.S. thesis, University College Dublin, Dublin, Ireland, (2012).

[12] D. F. Laefer, N. Ambrozevitch-Cooper, M. P. Huynh, J. Midgette, S. Ceribasi and J. Wortman, "Expansive fracture agent behaviour for concrete cracking", *Mag. Concr. Res.*, Vol. 62, No. 6, pp. 443–452, (2010).

[13] Y. F. Yapan, H. G. Korkmaz, S. Toros and M. Türköz, "Experimental and numerical investigation of the damage state of Ti-6Al-4V alloy sheet in the tensile test, hydraulic bulging, and hydroforming processes", *Int. J. Adv. Manuf. Tech.*, Vol.

[14] A. Hashemi, M. Hoseinpour Gollo and S. M. H. Seyedkashi, "Bimetal cup hydroforming of Al/St and Cu/St composites: adaptive finite element analysis and experimental study", *J. Mech. Sci. Technol.*, Vol. 30, No. 5, pp. 2217-2224, (2016).

[15] R. Hambli, "Comparison between Lemaitre and Gurson damage models in crack growth simulation during blanking process", *Int. J. Mech. Sci.*, Vol. 43, No. 12, pp. 2769-2790, (2001).

[16] A. A. El-Aty, Y. Xu, W. Xie, L. L. Xia, Y. Hou, S. Zhang, M. M. Ahmed, B. Alzahrani, A. Ali, X. Huang and A. S. Sobh, "Finite element analysis and experimental study of manufacturing thin-walled five-branched AISI 304 stainless steel tubes with different diameters using a hydroforming process", *Materials.*, Vol. 17, No. 1, p. 104, (2024).

[17] F. A. Ahamed and P. Chinnaiyan, "Studies on finite element analysis in hydroforming of nimonic 90 sheet", *Mathematics.*, Vol. 11, No. 11, p. 2437, (2023).

[18] M. Alizad-Kamran, M. Hoseinpour-Gollo, A. Hashemi and S. M. H. Seyedkashi, "Determination of critical pressure in analyzing of rupture instability for hydromechanical deep drawing using advanced yield criterion", *Arch. Civ. Mech. Eng.*, Vol. 18, No. 1, pp. 103-113, (2018).

[19] A. Hashemi, M. Hoseinpour Gollo and S. M. H. Seyedkashi, "Process window diagram of conical cups in hydrodynamic deep drawing assisted by radial pressure", *Trans. Nonferrous Met. Soc. China*, Vol. 25, No. 9, pp. 3064−3071, (2015).

[20] L. Jebri, T. Lazghab, M. Toumi and M. Soula, "The behavior and forming performance of vapor hydroforming process of thin aluminum sheets: Numerical and experimental analysis", *Adv. Mech. Eng.*, Vol. 14, p. No. 4, p. 16878132221089380, (2022).

[21] D. Marquez-Monje, R. Escribano-Garcia and O. Zubiri, "Characterization and finite element modeling of microperforated titanium grade 2", *Appl. Sci.*, Vol. 14, No. 17, p. 7903, (2024).

[22] K. Komori and K. Matsushima, "Predicting ductile fracture during biaxial sheet stretching using an ellipsoidal void model", *Theor. Appl. Fract. Mech.*, Vol. 118, p. 103215, (2022).

[23] F. Xue, Y. Yan and J. Kang, "Predicting forming limit diagrams for AZ31 magnesium alloy and 7050 aluminum alloy by numerical simulation", *J. Strain Anal. Eng. Des.*, Vol. 56, No. 8, pp. 598-608, (2021).

[24] A. Jalil, M. H. Hosseinpour Gollo, and S. M. H. Seyedkashi, "Process analysis of hydrodynamic deep drawing of cone cups assisted by radial pressures", *Proc. Inst. Mech. Eng. Pt. B J. Eng. Manuf.*, Vol. 231, No. 10, pp. 1793-1802, (2017).

[25] M. L. R. Meragalge and P. Gamage, "Finite element simulation model to predict the formability of AA 2014 T6 aluminum sheets at elevated temperatures". *Proc. 10th Int. Conf. Inf. Autom. Sustainability (ICIAfS)*, Negambo, Sri Lanka, pp. 542-547, (2021).

[26] A. Nakwattanaset and S. Suranuntchai, "Formability analysis on ultra-high strength steel for automotive parts using finite element simulation", *Mater. Sci. Forum.*, Vol. 1018, pp. 137-144, (2021).

[27] M. M. Shahzamanian, M. Parsazadeh, and P. D. Wu, "Numerical and analytical analyses of the formability and fracture of AA7075-O aluminum sheets in hemispherical punch tests," *Int. J. Solids Struct.*, Vols. 286–287, p. 112558, 2024.

[28] J. Zhang, "Numerical analysis and application of Marciniak and Nakazima experimental model on the formability of 304l Sheet," *J. Phys. Conf. Ser.*, Vol. 2834, p. 012152, (2024).

[29] T. S. Yang and J. Y. Huang, "Forming limit analysis of magnesium alloy sheet

metal forming process at elevated temperatures," *J. Phys. Conf. Ser.*, Vol. 2878, p. 012022, (2024).

[30] Y. Guo, T. L. Burnett, S. A. McDonald, M. Daly, A. H. Sherry, and P. J. Withers. "4D imaging of void nucleation, growth, and coalescence from large and small inclusions in steel under tensile deformation." *J. Mater. Sci. Technol.*, Vol. 123, pp. 168-176, (2022).

Copyrights ©2026 The author(s). This is an open access article distributed under the terms of the Creative Commons Attribution (CC BY 4.0), which permits unrestricted use, distribution, and reproduction in any medium, as long as the original authors and source are cited. No permission is required from the authors or the publishers.



How to cite this paper:

S. A. Alavi, S. M. H. Seyedkashi and M. Rakhshkhorshid, " Failure analysis of St12 steel during expansion forming by SCDA: a combined finite element and experimental approach", *J. Comput. Appl. Res. Mech. Eng.*, Vol. 15, No. 2, pp. 199-207, (2026).

DOI: 10.22061/jcarme.2026.12353.2702

URL:
https://jcarme.sru.ac.ir/?_action=showPDF&article=12594